AIAA JOURNAL
Vol. 42, No. 4, April 2004

Radio-Frequency Oxygen Plasma as a Sterilization Source

A. A. Bol'shakov,* B. A. Cruden,† R. Mogul,‡ M. V. V. S. Rao,§ S. P. Sharma,¶ B. N. Khare,** and M. Meyyappan††
NASA Ames Research Center, Moffett Field, California 94035

An oxygen plasma sustained at 13.56 MHz in a standardized reactor with a planar induction coil was used for biological decontamination experiments. Optical emission, mass spectrometry, Langmuir probe, and electrical measurements were applied to detection of chemical species and ion-energy and flux analysis. These diagnostics identified a plasma-mode transition in the range of 13–67-Pa pressure and 100–330-W power to the induction coil. At higher pressure and lower power, the plasma was sustained in a dim mode (primarily by stray capacitive coupling). A primarily inductive bright mode was attained at lower pressure and higher power. The coupling mode of plasma operation was then monitored by emission spectroscopy on an analogous, scaled-down reactor for biological degradation tests. Plasmid DNA degradation efficacies were compared in both plasma modes. DNA removal was ∼25% more efficient in the inductively coupled mode than in the capacitively coupled mode at the same power. The fast degradation was attributed to synergetic mechanisms (photo- and ion-assisted etching by oxygen atoms and perhaps O_2^* metastable molecules). Volatilization rates of the decomposition products (CO_2, CO, N_2, OH, H) evolving from the microbial (*Deinococcus radiodurans*) and polypeptide samples exposed to the plasma were compared. A plasma sustained in Martian atmosphere is considered.

I. Introduction

A MAJOR concern for exploration of other planets is the transport of biological contamination from Earth carried along with spacecraft. NASA planetary protection policy within the COSPAR international agreements tolerates no more than 300 bacterial spores per square meter on exposed surfaces of any extraterrestrial direct-contact lander, rover, or probe. Requirements for sample return missions or in situ identification of possible bio/organic traces on foreign planets are significantly stricter. Despite rigorous presterilization and all precautions, terrestrial microorganisms might remain in the interiors of spacecraft components, porous materials, cracks, and cervices. Hence, in-flight (on-board) removal of viable biological and organic matter from the sampling probe immediately before the sampling event gives the best guarantee of complete sterilization. This justifies the development of a low-power compact sterilizer that can utilize Martian atmospheric gas as a sterilizing agent.

As the Martian atmosphere consists of 95% CO_2 at ∼700 Pa, a plasma discharge produced in open atmosphere on Mars's surface will form a mixture of three major decomposition components (CO, O_2, CO_2). At a plasma gas-kinetic temperature around 600 K, CO_2 dissociation up to 80% is common and oxygen production can be as high as 30% (Ref. 1), so it is anticipated that production of an efficient sterilization plasma directly from the Martian atmosphere may be possible.

Received 20 November 2002; revision received 25 August 2003; accepted for publication 31 October 2003.

*Senior Research Associate, Space Technology Division; on leave from V. A. Fock Institute of Physics, St. Petersburg State University, 198904, St. Petersburg, Russia.

†Senior Scientist, Ames Center for Nanotechnology; bcruden@mail.arc.nasa.gov.

‡Faculty Fellow, Education Associates; currently Assistant Professor, Wilkes Honor College, Florida Atlantic University, Jupiter, FL 33458; mogul@fau.edu.

§Senior Project Scientist, Ames Center for Nanotechnology; contracted through ELORET Corporation, Moffett Field, CA 94035.

¶Senior Research Scientist, Space Technology Division; ssharma@mail.arc.nasa.gov. Associate Fellow AIAA.

**Senior Scientist, Space Science Division; also Research Scientist, SETI Institute, Mountain View, CA 94043; bkhare@mail.arc.nasa.gov.

††Scientific Director, Ames Center for Nanotechnology; meyya@orbit.arc.nasa.gov.

In recent years, low-power-driven plasmas have been found to be effective for sterilization of sensitive medical devices and electronic equipment.[2] Interest in plasma sterilization techniques for rapid and thorough biological decontamination protocols has been steadily growing. A substantial body of work on gas-discharge sterilizing effects in the pressure domain 0.1–1000 Pa has recently been reviewed.[3] Among plasmas in various gases, low-power discharges in carbon dioxide and oxygen were analyzed as sterilization means. Oxygen was found to be one of the best sterilizing agents. In parallel, a germicidal effect of plasmas in air (with or without additives) operating at terrestrial atmospheric pressure (100 kPa) has been extensively studied.[4] However, our considerations are restricted to the lower pressure case that is relevant to the Martian surface conditions.

Advantages of plasma treatment over other sterilization procedures (steam, dry heat, chemical disinfectants, or ultraviolet or gamma irradiation)[5,6] are low energy consumption and freely available reagents such as air or oxygen. Constraints imposed on biological and organic decontamination of Mars ascent vehicles necessitate complete and rapid removal of even the most robust microorganisms, which are resistant to high-radiation and vacuum environments. Various low-pressure plasmas in O_2, N_2, H_2, and mixtures thereof with CF_4 are routinely used for etching of photoresist and other organic polymers[7–11] at adequately high rates (up to 0.15 μm/s), which implies successful application of similar plasma tools in sterilization and removal of bio/organic traces. A number of studies have been specifically devoted to microbial inactivation during oxygen-plasma exposure.[3,12–22]

In one of the earlier works, oxygen in a flowing afterglow reactor at 30–130 Pa was less effective than helium and argon, probably owing to short lifetime of oxygen atoms in that design geometry.[12] Since then, several research groups[13–15] have used semiconductor etching or photoresist stripping equipment in plasma sterilization experiments with capacitively coupled rf or microwave plasmas at low pressure (≤10 Pa). Microbial spores exposed to oxygen plasma[14] exhibited greater etch resistance than organic polymers, owing to higher complexity in their structural macromolecules, multilayer coating architecture, and sophisticated morphology. Subramanyam et al.[16] found significant differences in plasma effects on different cultures of spores and germs. They compared microwave plasmas at 14 Pa in mixtures of Ar, O_2, H_2, He, and N_2 that produced the fastest inactivation by ionized atomic hydrogen (protons) due to their small size and, thus, the deepest penetration capability. At low pressures, reactive plasma components are sparse and ineffective.

In a parallel-plate capacitive discharge in air at 80 Pa, the main sterilizing mechanism was attributed to physical sputtering by accelerated ions.[17] In a microwave plasma at significantly lower ion

energies, chemically reactive oxygen species were found[14] as the main contributors to mortality and destruction of spores, but the sporicidal action of oxygen plasma under these conditions was not greatly affected by highly energetic ultraviolet photons radiated from the plasma. Little difference was noted between bactericidal efficacies of plasmas in O_2, CO_2, or mixtures of O_2 with H_2 and Ar. Hury et al.[15] observed that an electron cyclotron-resonance plasma with CO_2, H_2O, or H_2O_2 exhibited slightly higher destruction efficiency than an oxygen plasma, but all oxygen-based gases were more efficient than argon. They claimed that, under their conditions, degradation of microorganisms was a result of chemical attack by oxygen-containing radicals. Survivability of spores depended on density of population, so that isolated spores were less resistant than stacked or aggregated spores.

Moreau et al.[19] investigated procedures of spore inactivation in a flowing afterglow plasma with microwave excitation at pressures between 130 and 930 Pa. They found that the inactivation process occurs in three steps interpreted as follows: fast killing of the exterior microorganisms on the surface of a microbial film, slow removal of the dead exterior microorganisms covering lower-lying organisms, and finally, fast destruction of residual spores. These researchers determined that plasma from an O_2/N_2 mixture provided faster sterilization than 100% oxygen plasma. This effect was ascribed to the bactericidal role of UV photons originating from NO molecules formed in the discharge. Unfortunately, no consideration was given to the chemical reactivity of NO molecules, which are known to enhance etching rates in some processes.[23] Most recently, Philip et al.[22] confirmed the dominating role of UV radiation over reactive erosion in 2% O_2/N_2 plasma. However, this group[19,20,22] insisted that oxygen atoms effectively participate in chemical reactions with bacteria to form volatile products such as CO_2 and H_2O. Removal of spores by plasmachemical etching takes a longer time than just inactivation of their genetic material (e.g., by UV or H^+ influx), but erosion of the outer bodies in spore stacks is essential to accessing the lower layers for complete sterilization.

Soloshenko et al.[21] evaluated experimental sterilization efficacy of the glow discharge in oxygen, air, or nitrogen (<420 W, 10–33 Pa) with a numerical plasma model. They concluded that complete inactivation of sporulated *Bacillus subtilis* on open surfaces was readily achieved by oxygen radiation in the far UV region (<220 nm), but radiation at longer wavelengths was not effective. They emphasized that sterilization of complex surfaces, where parts of the sample cannot be directly irradiated by the plasma, was realized by neutral oxygen atoms and excited molecules $O_2(a^1\Delta_g)$ and $O_2(b^1\Sigma_g^+)$. Sterilization time depended inversely on plasma density and fluxes of the active species (O and O_2^*), whereas these fluxes increased linearly with input power but changed weakly with pressure under their conditions.

An overall conclusion from the investigations reviewed is that the biological degradation efficacy of the plasma can be increased when the plasma density of the ionized species is enhanced (despite the limited immediate role of the ions in the degradation process at pressures higher than 10 Pa). This enhancement is due to increased fluxes of the neutral chemically reactive atoms and excited molecules as well as more intense ultraviolet radiation in higher density discharges. Therefore, it is logical to employ a plasma in an inductively coupled mode, which provides higher density of electrons and ions than a capacitively coupled plasma at the same incident power.

We are not aware of any recent work on sterilization by inductively coupled plasma. Only initial experiments were accomplished using plasma reactors of cylindrical geometry with induction coils wrapped around the reaction chambers. Boucher[18] referred to the possibility of creating plasma by either inductive or capacitive coupling but placed the main focus of his invention on aldehyde additives to agent gases (oxygen, argon, or nitrogen) activated in rf or microwave discharges. No systematic study was conducted on the distinction between sterilizing efficacies of plasmas sustained in inductive and capacitive regimes.

Thus, the present research is focused on application of oxygen rf plasmas in inductive vs capacitive mode for sterilization purposes and comparison between efficacies of plasmas in oxygen and Martian-atmosphere-analog gas. Of particular importance is the sterilization of highly desiccation- and radiation-resistant microorganisms that can survive the low-pressure and intense-radiation environments of interplanetary space and on the surface of Mars. Included in the study is a particularly resistant terrestrial biological model, the microbe *Deinococcus radiodurans*, which can survive in radiation environments of up to 6000 rad/h.[24,25] Hence, a specific objective of this study is to address the efficacy of low-power rf discharges for plasmachemical degradation of microorganisms with resistance to ultraviolet radiation and reactive media.

II. Experimental Setup

Two independent plasma reactors were employed in this work. Studies on microbe cell, protein, and deoxyribonucleic acid (DNA) degradation were performed using a home-built biological decomposition reactor. Relevant plasma diagnostics were carried out in a separate reactor with several diagnostic tools attached. Both reactors featured a planar spiral coil electrode on the top of the plasma chamber and a grounded water-cooled bottom electrode. Upper electrodes in both reactors were driven by rf power at the standard frequency of 13.56 MHz. The reactor used for plasma diagnostics was a modified (inductive) Gaseous Electronics Conference (GEC) reference cell along with the attached diagnostic equipment described earlier.[26] The biological degradation reactor consisted of a main reaction chamber, which was essentially a scaled-down version of the GEC cell, and an additional sample-loading chamber with a vacuum-tight gate separating the two chambers.[27] This design facilitated rapid introduction of the biological samples and simultaneously allowed stable plasma conditions to be preserved throughout the course of experiments.

In both reactors, induction coils were insulated from the plasma by flat quartz plates. The GEC cell's lower electrode was integrated both mechanically and electrically with a high-transmission electrostatic-quadrupole plasma analyzer (EQPA) from Hiden Analytical. A 10-μm hole in the center of the GEC cell's lower electrode served as the ion-sampling orifice for the EQPA. In the biological degradation reactor, the samples were placed on the grounded bottom electrode, which was in direct contact with the plasma. To measure the temperature of the exposed electrode surface, a thermocouple was installed in the center of the lower electrode. Reagent gas was flowed through the reactors at constant flow rates ($\sim$10 cm^3/min in the GEC cell and $\sim$100 cm^3/min in the biological degradation reactor).

Emission spectra from the plasma were collected through quartz (GEC cell) or Pyrex (biological degradation reactor) windows by a quartz lens and recorded using a SpectraPro 300i 0.3-m spectrograph (Acton Research) and a SpectruMM 1024 $\times$ 250 back-illuminated charge-coupled device camera (Roper Scientific). A holographic grating (1200 gr[grooves]/mm) allowed capture of the spectral range 180–940 nm with average inverse linear dispersion of the system equal to 2.7 nm/mm. Slit widths from 0.1 to 0.25 mm were used.

The impedance and other electrical characteristics of the plasma were measured by a plasma impedance monitor (PIM) from Scientific Systems mounted in line with the induction coil. An rf-compensated Langmuir probe (Smart Probe from Scientific Systems) was used[26] to measure the plasma parameters, such as ion number density n_i, electron number density n_e, and electron temperature T_e.

Deinococcus radiodurans was obtained from the American Type Culture Collection and stored as glycerol stocks at -193 K. Bacterial growth media were prepared using reagents purchased from Sigma Co. Plasmid DNA (pRc/CMV2) and bovine serum albumin protein (BSA) was also purchased from Sigma Co. DNA molecular weight standards were obtained from Invitrogen. Oxygen was supplied by AirGas (99.9%) and Scott Specialty Gas (99.99%). Martian-atmosphere-analog mixture containing 95.48% CO_2, 2.51% N_2, and 2.01% Ar was obtained from Matheson Gas. Hanging drop slides were obtained from Fisher Scientific. Deionized high-purity water (18 MΩ/cm) was used for sample preparation.

III. Technical Approach

A. Sterilization Experiments

Prior to introduction of the biological sample, the pressure in the load chamber was reduced to 2–3 Pa and plasma was ignited. Then reagent gas was added to the target pressure of 13 or 67 Pa. The reaction chamber gate was then opened and the sample was shifted into the plasma discharge in the main reaction chamber. After being exposed to the plasma, the sample was shifted back to the load chamber, the gate was closed, and then the load chamber was filled up to 100 kPa (1 bar) with dry air. The sample was then removed and analyzed using microbiological and biochemical techniques. Throughout the experiments, the plasma remained running and stable, allowing acquisition of reproducible data.

The effect of plasma exposure on DNA was assayed by studying the relationship between the degree of DNA degradation and discharge parameters such as rf power, pressure, and reagent gas. Plasmid DNA (pRc/CMV2, 5.5 kb) was dissolved in water to 0.5 μg/μl and added onto hanging-drop slides in 2-μl aliquots. The slides were dried under moderate vacuum, transferred to the biological degradation reactor, and exposed to a 250-W oxygen plasma at 13 and 67 Pa for 5 and 20 s. Several control experiments were also performed by 1) analyzing the untreated DNA samples and by 2) heating the dried DNA samples to ~370 K at 13 Pa for 20 s. After exposure, each sample was dissolved in 12 μl of 25 mM HEPES (*N*-[2-hydroxyethyl]piperazine-*N*′-[2-ethanesulfonic acid) (pH 8.0) and 10 μl was transferred to a 1.5-ml tube containing 2 μl of 6 × DNA running dye. All samples were analyzed in parallel by electrophoresis at 80 V using a 0.8% agarose gel with 0.25 μg/ml ethidium bromide in *tris*-acetate/EDTA (ethylenediaminetetraacetic acid) buffer.

The volatilization of model protein and microbe exposed to the plasma was monitored with emission spectroscopy. Dried protein and microbial films were prepared using BSA and *D. radiodurans*. BSA was dissolved in water to 100 mg/ml, and 10 μl was transferred to a hanging drop slides. Slides containing 1 mg BSA were dried and exposed to the oxygen plasma. Two fresh samples of *D. radiodurans* were prepared from mid-log-phase cultures by removal of 2-ml aliquots followed by harvesting in a 14,000-rpm centrifuge for 30 s. Each cell pellet was thoroughly resuspended with 1 ml of water and then harvested and the procedure was repeated three times. The washed cell pellets were resuspended in 30 μl of water, transferred to hanging drop slides (~10^9 total cells), and dried under moderate vacuum. A control sample was prepared using 30 μl of pure water. Exposure of each sample to the oxygen plasma was performed at 100 W in a closed (nonflowing) reactor using oxygen as a reagent gas at an initial pressure of 67 Pa. During the course of the microbial exposure, the pressure within the reaction chamber rose about 20 Pa, indicating rapid conversion of the biological matter into the gaseous phase. The emission spectra of the plasma discharge were recorded immediately upon exposure of the sample and repeated at 3–10-min intervals over the course of ~40 min. Spectra of decomposition products from duplicate microbial samples were compared for reproducibility and against the pure water control for any background contamination.

Plasmas in oxygen and in a Martian-atmosphere-analog mixture (95.3% CO_2, 2.5% N_2, 2.0% Ar) were compared at 67 Pa and power levels from 50 to 200 W for 60 s each. The samples were introduced and analyzed as described above. Agarose gels were visualized by fluorescence excited at 302 nm; the images were captured and the DNA bands quantified using a laboratory imaging and analysis system (UVP, Inc.). The DNA sizes were estimated by comparison to a 1-kb DNA molecular weight ladder and the percent change in each DNA band was calculated by comparison to the untreated control. All reactions were done in duplicate.

B. Plasma Characterization Experiments

Procedures for the analysis of ion fluxes, ion energy distributions, Langmuir probe, and PIM data have been described previously.[28] Ion densities were calculated using the standard Laframboise formula with an effective mass found from the balance of the ion fluxes measured experimentally. The efficiency of power utilization, or fraction of power deposited into the plasma (as opposed to being dissipated in the circuitry), was determined by the equivalent resistance method.[29,30] It is assumed in this approach that the stray power consumption in the matching network and inductive coil can be described by a single equivalent resistance in series with a nonlossy transformer circuit. The power loss in the matching network is a function of the current to the coil. Therefore, stray power loss was determined using the current measured by the PIM. The power deposited into the plasma was assumed to be the difference between applied power and this loss.

The rotational temperatures of the oxygen molecule and molecular ion were estimated by fitting the emission bands of the $O_2 b^1\Sigma_g^+ - X^3\Sigma_g^-$ and $O_2^+ b^4\Sigma_g^- - a^4\Pi_u$ systems. The fitting procedure was similar to that employed earlier.[31] The O_2 spectrum in the 754–774-nm range included simultaneous fits of the (0,0), (1,1), and (2,2) bands for rotational and vibrational temperature using the upper state rotational constants of Cheah et al.,[32] the lower state constants of Rouille et al.,[33] and the Franck–Condon factors of Krupenie.[34] In intensity calculations, the formulae of Watson[35] for a magnetic dipole transition were appropriately modified for the triplet state being the lower state. The rotational temperatures reported for O_2^+ represent the weighted averages of three different fits, involving bands described by vibrational quantum numbers (v, v) for $v = 0, 1, 2, 3$ between 575 and 610 nm, $(v+1, v)$ for $v = 0, 1, 2$ between 545 and 565 nm, and $(v+2, v)$ for $v = 0, 1$ in the range of 510–540 nm. For these fits, the Dunham coefficients from Albritton et al.[36] were used to determine rotational constants and Krupenie's Franck–Condon factors were used for vibrational populations. For the intensity determinations of rotational lines, the approach of Hill and Van Vleck[37] was employed starting from a Hund's case (a) basis set. Correctness of the fitting procedure was verified through comparison to intensities fit in the (3,1) band by Albritton et al.[36] The vibrational temperatures are considered as fit parameters to match relative intensities of overlapping bands but are not believed to represent any physically meaningful temperature. Therefore, only rotational temperature values are reported here.

Significant effort in this work was focused on using diagnostics to identify the transition between inductive and capacitive modes of operation. These modes differ in particular by higher ionization degree in inductive mode but higher electron and ion mean energies in capacitive mode. While in our setup the rf power was coupled to the plasma by an inductive coil, large voltages on the coil often resulted in sufficient electric field between the coil and the grounded surfaces to sustain a discharge in a capacitive mode.

IV. Results and Discussion

A. Plasma Coupling Identification

The emission spectra of the 100% oxygen plasma and the plasma in Martian-atmosphere-analog mixture were recorded under various conditions. A plasma ignited in the Martian-atmosphere analog revealed a multitude of excited species such as CO_2^+, CO, CO^+, N_2, N_2^+, Ar, and atomic oxygen. The oxygen-plasma spectra[27] generally resembled previously published oxygen spectra,[38,39] including O and O^+ lines and molecular bands from O_2 and O_2^+. Advantageously for this emission spectroscopic study, the 100% oxygen plasma exhibited only a low background in the region between 180 and 400 nm, so that identification and monitoring of the reaction by-products during biological degradation in the plasma were simplified. In contrast, the plasma in Martian-atmospheric-gas analog presented a significantly higher integrated intensity of the congested spectrum in the 180–380-nm range but lower intensities of oxygen spectral lines as compared to the 100% oxygen plasma. Thus, the plasma in oxygen was used in most of our experiments.

At higher pressures (40–67 Pa) and lower powers (100–165 W), the oxygen plasma in both reactors was sustained in a dim mode, in which discharges were primarily coupled to the incident rf field through stray capacitance between the coil and interior ground surfaces. This regime was characterized by slow decrease in emission intensities of all excited species (except O_2^*) with increase in pressure, as is common for capacitively coupled discharges.[40] The absolute intensities of atomic and molecular ions (O^+ and O_2^+) remained

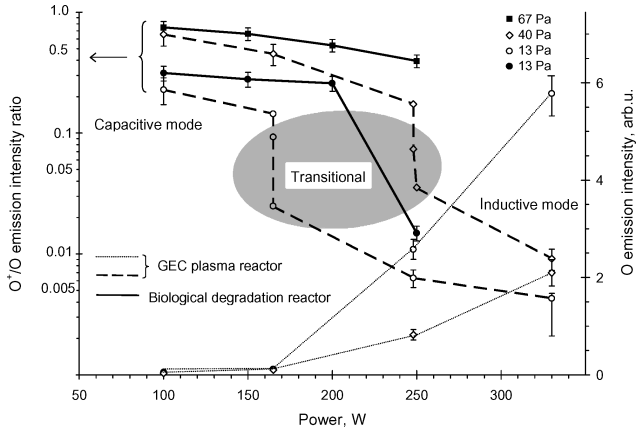

Fig. 1 Ratio of emission intensities for the atomic oxygen ion (435 nm) and neutral atomic oxygen (927 nm) for two pressure cases in the two reactors. The inductive mode is characterized by a significant change in this ratio due to an increase in oxygen dissociation and a decrease in the density of high-energy electrons (drop in T_e). The gray indicates a transitional region of partially inductive coupling with a capacitive component. Dotted lines represent relative intensities of the oxygen emission at 927 nm in the GEC reactor. Open (solid) markers correspond to data from the GEC reactor (biological degradation reactor).

at comparable levels. When the incident rf power was increased up to or above 250 W, a transition into a bright, primarily inductive coupling mode was obtained. These capacitive (dim) and inductive (bright) regimes are sometimes called E and H modes of the discharge, respectively. Increasing atomic oxygen emission with increased rf power is illustrated in Fig. 1 by dotted lines.

For the biological degradation reactor, primarily inductive coupling was realized only at the lowest examined pressure (13 Pa) and a relatively high power (250 W). Under all other experimental conditions, the plasma remained in a dim mode, coupled through the stray capacitance of the system. The degree of capacitive coupling is in part determined by the proximity of grounded surfaces to the induction coil. The grounded surfaces were closer to the coil in the biological degradation reactor than in the GEC cell. Nearer ground sources give a greater stray electric field at otherwise similar coil voltages. The result was that the biological degradation reactor favored a capacitive mode of operation at conditions otherwise identical to these in the GEC cell. This is why the inductive mode was only obtainable at the extreme of pressures and powers explored with the biological degradation reactor.

For the GEC reactor, a very sharp transition from stray capacitive coupling to clear inductive coupling was observed at a lower pressure (13 Pa). As rf power was increased from 100 to 250 W and higher, the intensities of atomic spectral lines increased by one or two orders of magnitude. The most considerable change was for those oxygen lines that originated from highly excited atomic energy levels. This effect was attributed to a combination of significantly higher electron number density and higher atomic oxygen density in the inductively coupled mode than in the capacitive mode. At the same time, the ionic (O^+) spectral lines decreased in intensity to well below the O_2^+ emission intensities. The latter resulted from reduction in the number of fast electrons capable of exciting the atomic ions (excitation thresholds above 25 eV) despite the increased absolute ion density in the plasma.

The difference in emission intensities originating from the neutral atoms and atomic ions at the transition between capacitive and inductive modes of plasma operation was the most pronounced. Other emitting species exhibited a relatively moderate change in their intensities. Therefore, the ratio of intensities of ionic to neutral atomic spectral lines was used as an indicator of the mode of plasma coupling. The magnitude of this ratio for both reactors is plotted in Fig. 1 vs the rf power that was applied to the plasma. Based on the ratio of O^+ to O line intensities, three ranges of plasma regimes were identified: capacitive, transitional, and inductive. They are schematically depicted in Fig. 1.

Subsequently, an extensive array of plasma parameters were measured in the GEC reactor to verify and fully characterize these regimes of plasma operation. It was then inferred that a change between solely capacitive and clearly inductive coupling modes was not always a steplike transition. Depending on conditions, a nonabrupt but irregular transition was also possible, reflecting an increase in capacitive coupling while still in the inductive mode. Such transitional behavior in electronegative gases was predicted and measured by other researchers.[41]

The electron and positive ion number densities (n_e, n_i) and electron temperature measured by the Langmuir probe are plotted in Fig. 2. Both n_e and n_i increased with power, as expected. This dependence was stronger at lower pressure. The positive ion density was high ($>3 \times 10^{11}$ cm^{-3}) in inductive mode but about one order of magnitude lower ($\sim 3 \times 10^{10}$ cm^{-3}) in capacitive mode. The electron densities were generally less than the positive ion densities (due either to the presence of negative ions in the plasma, as predicted by the model,[42] or to failure of commonly applied assumptions[43,44] in calculating ion density from Langmuir probe data). The magnitude of the electron temperature was relatively high in the primarily capacitive mode ($T_e = 5.4$ eV at 40 Pa, 165 W) and decreased with increasing power as a result of enhancement in inductive coupling. In the primarily inductive mode, the electron temperature was low ($T_e \approx 3$ eV at 13 Pa), in agreement with the results from similar inductively coupled plasmas.[45]

Figure 3 shows total positive ion flux to the bottom electrode as a function of rf power for 13 and 40 Pa in the GEC cell. The total positive ion flux intensified with increased rf power. A fivefold amplification in the ion fluxes at 13 Pa was a result of the transition into an inductive mode of operation at higher power. The ion energies in this inductively coupled regime (13 Pa, 250–330 W)

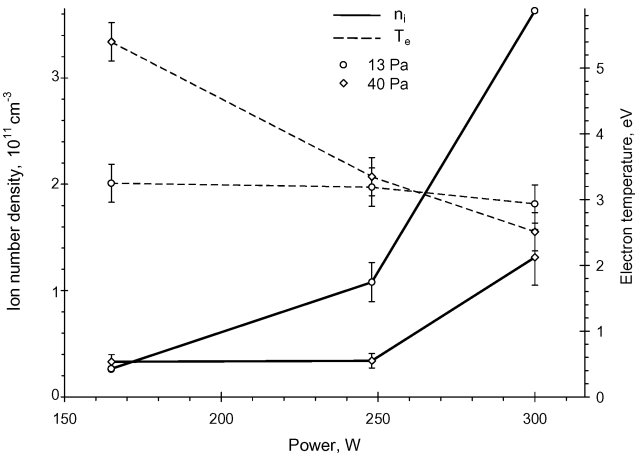

Fig. 2 Langmuir probe measurements of the positive-ion densities and electron temperature at 13 and 40 Pa in the GEC cell.

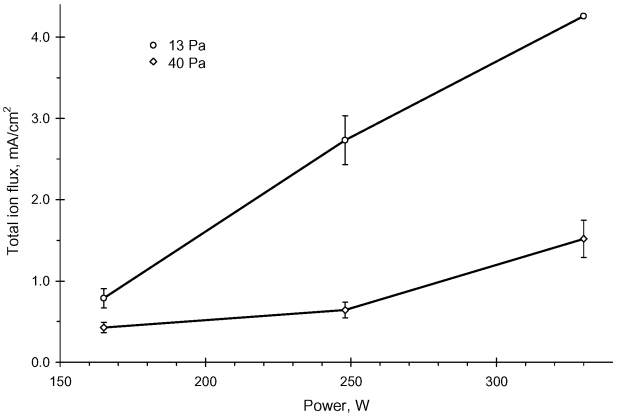

Fig. 3 Total positive-ion flux measured by mass spectrometry in oxygen plasma as a function of rf power for 13 and 40 Pa.

were much lower and less dispersed than those at 40 Pa, as shown in Fig. 4 for O^+ ions. At the lower power (<250 W) under 40-Pa conditions, the plasma appeared not to have attained an inductive discharge; the ion fluxes were relatively small and grew only moderately with power. In the latter case, the ion energy distributions had kinetic energies broadly ranging from 30 to 70 eV, dependent upon power, thus indicating capacitive coupling with significant rf modulation of the plasma sheath near the grounded electrode surface.

For most of the conditions, the O^+ ions on average were slightly more energetic than the O_2^+; otherwise both ions, O^+ and O_2^+, behaved similarly. In addition, doubly ionized O^{2+} ions were observed at 13 Pa, and ozone ions O_3^+ were detected at 40 Pa, but their densities were negligible compared to those of O_2^+ and O^+. Hence, the sum of the results illustrated in Figs. 2–4 was considered sufficient for characterization of the major ions under conditions relevant to the present study. This ion analysis complemented and confirmed distinctions made between the coupling modes of plasma operation based on the optical emission observations (Fig. 1).

The plasma impedance was also estimated as the most decisive criterion for determining the nature of the plasma coupling. The imaginary impedance always appeared to be negative, implying a significant stray capacitance of the GEC reactor. At lower pressure and higher power, a decrease in the scalar value of imaginary impedance was observed. This indicated a reduction of the stray capacitance and transition into inductive mode. In all cases of inductive coupling, plasma showed nearly the same imaginary impedance. Consistent with these results were estimates of the power-coupling efficiency, shown in Fig. 5 along with the induction coil voltage values. Under stray capacitative coupling, the voltage (and resistive loss) on the coil was high and coupling efficiency was as poor as 40%. The primarily inductive coupling produced lower coil voltages and showed a significantly higher efficiency, with about 80% of the power going into the plasma.

In the capacitive mode, the ion densities were low but their energies were high. Thus, a significant fraction of the applied rf power had to be wasted in accelerating ions to make this regime self-sustaining. Furthermore, the poor coupling efficiency caused deflection of some power into resistive heating of cables and circuitry. In the inductive mode, more energy was deposited into ionization processes, creating higher ion and electron densities and greater dissociation of O_2, along with an increase in overall rates of all electron impact processes. The bright, primarily inductive coupling mode provided higher ion and photon fluxes, particularly to the surface of the bottom electrode where biological samples were deposited. These effects were beneficial for biological decontamination. The efficiency of power coupling in the inductive mode was also higher than that in the capacitive mode. Clearly, all issues related to the efficiency of power utilization are critically important for extraterrestrial applications.

B. Degradation of Biological Matter

The differences in plasmid DNA degradation by exposure to inductively or capacitively coupled plasma modes were assayed using agarose electrophoresis analysis of the reaction products. Each plasma exposure was performed at identical power (250 W) but at differing pressures (13 and 67 Pa) for the inductive and capacitive modes. The results in Figs. 6 and 7 demonstrate that inductively

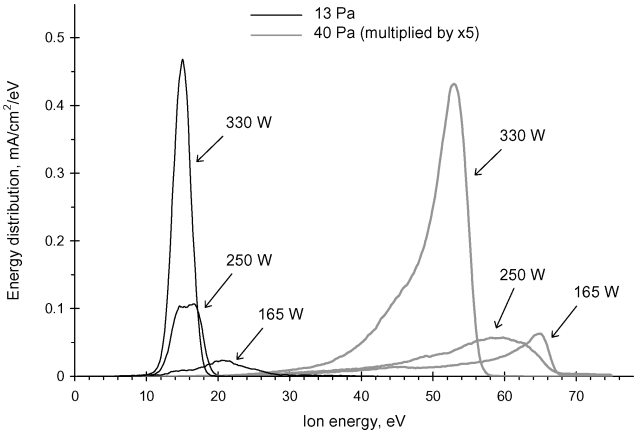

Fig. 4 Ion energy distributions of atomic ions O^+ for a set of power levels (165, 250, 330 W) at 13 and 40 Pa in the oxygen plasma. Signal values for 40 Pa were multiplied by a factor of 5.

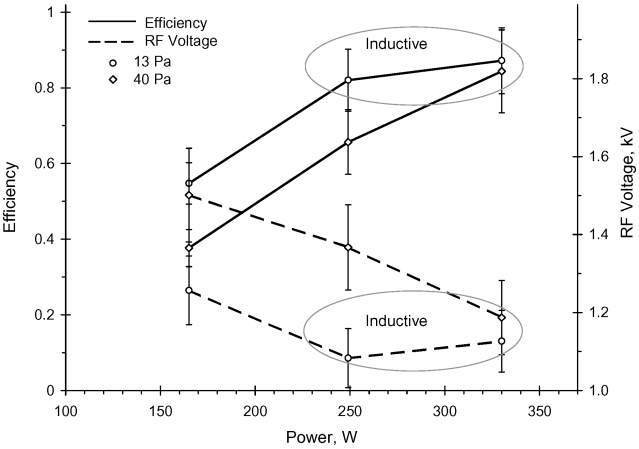

Fig. 5 Estimated coupling efficiency and magnitude of rf voltage on the coil. Regions believed to be characteristic of inductive coupling are indicated.

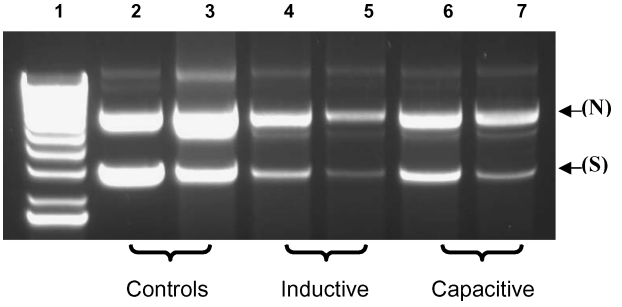

Fig. 6 Degradation of DNA by oxygen plasma in inductive and capacitive modes at 250 W. Supercoiled and nicked plasmid DNA are labeled as (S) and as (N), respectively. Lane 1, 1-kb DNA ladder; lane 2, untreated DNA; lane 3, DNA thermal control; lane 4, 5 s, 13 Pa; lane 5, 20 s, 13 Pa; lane 6, 5 s, 67 Pa; and lane 7, 20 s, 67 Pa.

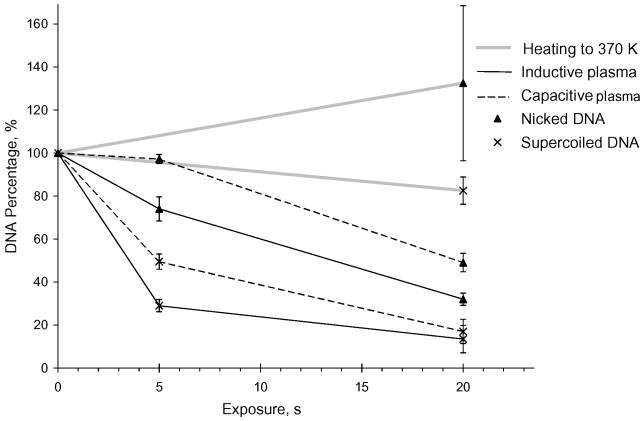

Fig. 7 Quantification of the results from Fig. 6 for a comparison of DNA destroyed by exposure to oxygen plasma at 250 W and pressures of 13 Pa (inductive mode) and 67 Pa (capacitive mode).

coupled plasma destroyed over 70% of the supercoiled DNA in 5 s but capacitatively coupled plasma only 50%. The capacitively coupled plasma required a longer time for higher degradation. The degradation rate of nicked DNA during the first 5 s in the capacitive mode was ~10-fold inferior to that in the inductive mode. The plasma exposure caused backbone fragmentation, forming new products, such as linearized plasmid DNA and low-molecular-weight DNA fragments.[27] The original DNA and its fragments were further reduced via volatilization. For all samples, the faster degradation rates were achieved with inductive coupling.

The DNA samples overexposed to plasma in a capacitative mode were chemically converted into a brown residue that was insoluble in water. The residue could result from extreme damage inflicted by the highly accelerated ions. In contrast, the exposure to plasma in an inductive mode yielded no visible residue, owing to higher density of atomic oxygen available for sample removal and lower energy of the ions. This difference suggests that the inductive mode was capable of thorough DNA decomposition into volatile components and was better suited for the complete removal of DNA or other biomolecules.

For a comparison of plasma-based vs thermal degradation, a sample of DNA was heated to ~370 K for 20 s. Supercoiled DNA decreased slightly, whereas nicked DNA increased due to heat-induced fragmentation of the supercoiled plasmid (Figs. 6 and 7). The effect of thermal degradation at 370 K was considered not to be significant relative to the plasma exposure. During the plasma treatment, the DNA and other biological samples were deposited on the stainless-steel electrode, temperature of which was measured against rf power applied to the reactor. As shown in Fig. 8, this temperature was never higher than 370 K (however, sample temperature was not exactly the same as electrode temperature).

The main volume of the plasma was significantly hotter than the sample surface. The maximum temperature within the plasma volume was estimated as the rotational temperature derived from the molecular emission spectra. The calculation results for both reactors are represented in Fig. 9. The rotational temperature obtained from spectra of the neutral molecule O_2 was in the range 320–750 K, whereas the temperatures exhibited by the molecular ion O_2^+ were slightly higher at 370–1170 K (ion data not shown). For the biological degradation reactor, the emission spectra displayed a dependence on temperature that increased with power and pressure. In the GEC reactor, dependence on pressure was weaker. Conditions with the signature of inductive coupling were characterized by rotational temperatures above 550 K (with the exception of one data point).

To characterize decomposition of biological matter during the plasma exposure, the emission spectra were recorded from 280 to 940 nm. Shorter wavelengths were absorbed by the Pyrex window of the plasma reactor. Several sets of emission spectra from biological samples and control blanks exposed to the oxygen plasma (13 and 67 Pa; 100–250 W) were recorded. Spectra collected in

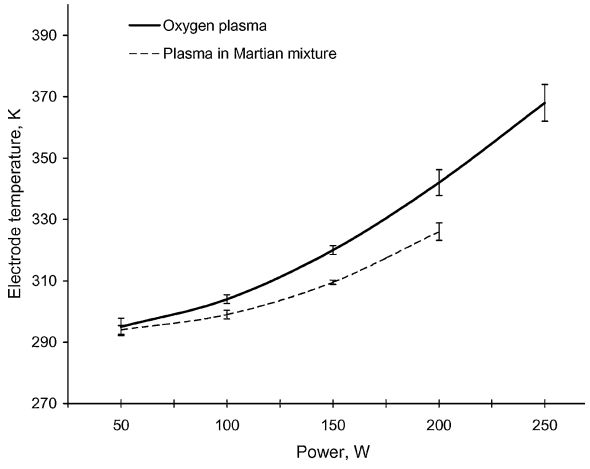

Fig. 8 Temperature of the lower electrode as a function of rf power applied to the biological degradation reactor.

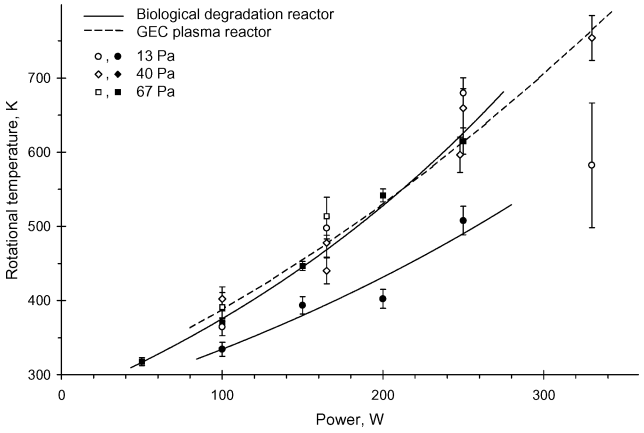

Fig. 9 Rotational temperature estimates of the oxygen molecule in the GEC cell (open markers) and biological degradation reactor (solid markers).

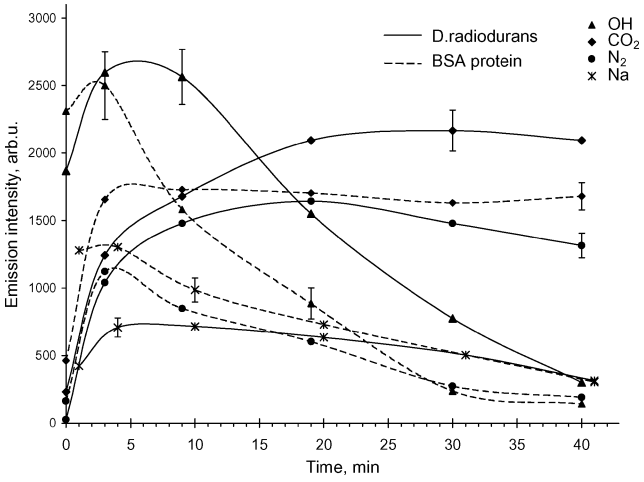

Fig. 10 Temporal change in emission intensities from the biological decomposition products during the exposure of *D. radiodurans* and BSA protein to the oxygen plasma at 67 Pa and 100 W (capacitive mode).

control experiments with pure water blank samples and microscope glass slides indicated no significant contamination resulting from the sample preparation, glass surfaces, or water stock, thus ensuring a low (undetectable) level of background contamination during the sample preparation phase.

Upon introduction of a biological sample, the products of sample decomposition evolved rapidly. The detected species were CO_2^+, CO, N_2, N_2^+, OH, H, Na, and K. These decomposition spectra, along with blank oxygen-plasma spectra recorded under our conditions, have been published elsewhere.[27] Intensities of oxygen species were monitored and remained stable during the biological degradation experiments. An exception was the molecular oxygen band $b^1\Sigma_g^+$–$X^3\Sigma_g^-$ around 763 nm. The intensity of this band decreased significantly after introduction of biological samples. The latter effect should probably be attributed to quenching of excitation by the products of decomposition. The absolute density of molecular oxygen was not affected.

The temporal evolution of the decomposition products during the exposure of *D. radiodurans* and BSA protein is displayed in Fig. 10. The changes in emission intensity of the degradation products were plotted vs time and normalized for legibility. No assumption regarding concentrations of the species should be made on the basis of data presented in Fig. 10. However, one can infer that the OH radical was the fastest to emerge from the oxidizing plasmachemical reactions. Temporal behavior of atomic hydrogen (not shown) was almost identical to that at OH, which suggests a very close relationship of these two species in a plasma. The formation of OH may result from reactions of oxygen with H atoms in the biological

macromolecules, thus yielding water and/or the hydroxyl radical. It is also possible that these are signs of residual water in the sample that was not removed during drying. The sample holder, when exposed to the plasma by itself, produced a barely detectable emission of OH.

The main observed product of decomposition of the biological matter was CO_2. Carbon monoxide evolved to a smaller extent and closely followed the temporal changes of the CO_2. Nitrogen was released from biomolecules in the form of N_2. The nitrogen molecule is the only thermodynamically stable form of nitrogen within a temperature range that occur in our experiments. It is evident from Fig. 10 that the total hydrogen and nitrogen content of the samples was volatilized faster than the carbon content. The latter fact was easily observable even without spectroscopic tools: a carbonaceous layer was the last residue of the samples to be removed. The microbial samples were more resistant to oxygen plasma than the BSA protein; i.e., the degradation rate of the latter was faster. Content of sodium and potassium was higher in BSA than in the *D. radiodurans* samples (potassium exhibited a strong integrating effect of "memory" of the history of previous sterilization experiments).

Emission spectroscopy is not an appropriate technique for detection of water vapor in the plasma, as the H_2O molecule is known to be a very weak emitter in routinely accessible wavelength regions. However, it is deducible from the degradation experiments presented here that hydrogen originating from biological samples was ultimately converted into water, carbon was converted into CO_2 and CO, and nitrogen was removed in the form of N_2. These plasma-assisted reactions closely resemble the polymer-etching process in the semiconductor industry.[11] Metals apparently originated from the salts included in the biological samples.

This low-temperature plasma sterilization process is similar to the flame combustion process at low pressure.[46,47] In flames, detectable quantities of the CN, CH, and NO radicals are formed. Volumetric concentrations of these species in flames (without nitrogen-rich fuels) were found to be in the range 5–100 ppm. However, none of these species (CN, CH, NO) was detected in the present study. These diatomic molecules are strong emitters and would have been detectable if their concentrations in oxygen plasma were above the detection limit of emission spectrometry (typically[48] a few ppm). Therefore, the CN, CH, and NO molar concentrations were generally below $\sim$1 ppm (their densities $<3 \times 10^{10}$ cm^{-3}) during plasma sterilization. The primary parameter that affects the formation rates of these radicals is the temperature. Our plasma gas temperature was always below 1000 K, while it reaches more than 2000 K in flames at low pressure.

C. Mechanisms of Sterilization by Plasmas in Oxygen and Martian Analog Gas

Several important mechanisms occur in the plasma sterilization process. These include 1) chemical reactions, e.g. with atomic oxygen, 2) UV-induced damage or photodesorption, and 3) ion sputtering. Most likely, these processes act synergistically, as typically occurs in semiconductor etchers, where material removal by combined chemical and ionic species is significantly faster than removal by either species alone.[40] Similarly, a synergetic effect has been proposed for UV-assisted chemical etching.[49] Several studies[3,20,21] have reported that UV radiation plays a major role in biological sterilization, particularly at low pressure. These studies characterized the UV effect in terms of microbial mortality rather than biomaterial degradation and removal efficiency. Chemically reactive species, such as O, are required for removal of biological matter (conversion into volatile byproducts: CO_2, CO, H_2O, and N_2). This removal may be enhanced by a flux of UV photons and/or ions to the surface to be cleaned from biological contamination.

The primary role of chemical reactivity in degradation of plasmid DNA is illustrated in Fig. 11. The percentage of removed supercoiled DNA and plasma emission data are plotted against power. Shown are the intensity of the O_2 band at 754–774 nm and the ratio of atomic O emission at 927 nm to this O_2 band emission. In a crude approximation, this ratio should be roughly proportional to the ratio of O to O_2 densities, since both atomic and molecular emissions are induced

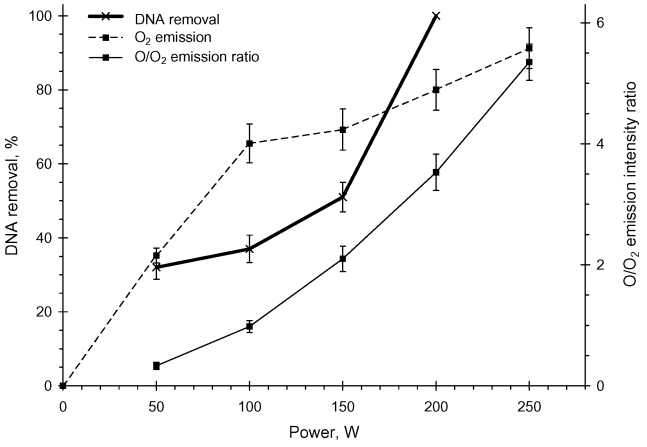

Fig. 11 Plot of DNA removal percentage, integrated O_2 (0,0) $b^1\Sigma_g^+$–$X^3\Sigma_g^-$ band emission intensity, and ratio of O (927 nm) to O_2 (atmospheric band) intensities vs power in the biological degradation reactor. The O_2 emission is assumed to be representative of vacuum UV radiation, and the O/O_2 ratio is assumed to be representative of atomic oxygen concentration.

primarily by electron impact on ground-state species and electron temperature does not change drastically within the range explored. With this assumption, the atomic O density depends superlinearly on power, whereas major molecular UV emissions should rise approximately linearly. The degradation curve exhibited a superlinear dependence on power that suggests the greater role of oxygen atoms than of UV radiation for DNA removal.

A comparison of biological effects of the discharges in Martian-atmosphere-analog mixture vs those in oxygen further emphasized the significance of reactive oxygen species. Atomic oxygen density in 100% oxygen plasma was roughly an order of magnitude higher than that in Martian-mixture plasma, as the analysis of the intensities of atomic spectral lines indicated. Experiments at equal exposures demonstrated that *D. radiodurans* samples were considerably less degraded by plasma in Martian atmospheric mixture than by oxygen plasma, whereas the DNA removal rates were only slightly lower. In terms of removing DNA and *D. radiodurans*, the plasma in Martian atmospheric mixture was less efficient than the 100% oxygen plasma, but the former caused more damage (fragmentation and cross-linking) to bare DNA.[27] This dissimilarity originated from the differences in the balance between fluxes of the chemically reactive species (atomic O) and ultraviolet radiation provided by discharges in the two gas media (Martian-analog mixture vs oxygen).

Under our conditions, the CO $A^1\Pi$–$X^1\Sigma^+$ band system dominated over emission spectrum of the plasma in Martian-atmosphere-analog mixture. This system is known to extend into the vacuum UV region with maximum emission at 149 nm and very strong bands within the range 140–230 nm.[50] Contributions from CO^+ and CO_2^+ emissions and several other CO band systems made the plasma in Martian atmospheric mixture a source of intense ultraviolet radiation in the 140-360 nm range. In oxygen plasma, the most intense emitters were the Schumann–Runge O_2 band system ($B^3\Sigma_u^-$–$X^3\Sigma_g^-$), with a maximum at 175–185 nm,[34,51] and atomic oxygen lines between 115 and 135 nm, including the resonance triplet at 130 nm. Direct measurement of the total ultraviolet emissions from the plasmas was obstructed by the opacity of the reactor windows at shorter wavelengths, thus only qualitative evaluations were made.

Spectra from the biological degradation reactor recorded within a Pyrex transparency yielded that the atomic O infrared lines (777, 845, 927 nm) were at least several times as intense as any of the observable CO or CO_2^+ bands. Obviously, the resonance lines of O atoms should be significantly more intense than these infrared lines and, therefore, more intense than spectral features of the CO/CO_2 species. This implies that oxygen atoms were stronger UV emitters in terms of both absolute spectral intensities and the energy of photons (shorter wavelength) than the carbon oxide species. However, the integral radiance emitted by the CO, $CO,^+$ and CO_2^+ species in

the UV region may be comparable to or greater than that emitted by the oxygen species.

As energy of photons depends inversely on wavelength, the damaging power of the photons increases in general at shorter wavelengths. At least 4.29 eV of energy is required for breaking C−H bonds, hence only photons at 289 nm and below can directly break them. Photons at wavelengths shorter than 196 nm are capable of breaking C=C and C=N double bonds. The bactericidal effect of plasma radiation was found to be strong at wavelengths shorter than 220 nm but insignificant at longer wavelengths.[21] DNA has an absorption maximum at around 260 nm due to absorption by the nucleotide bases.[52] Emissions at wavelengths below 200 nm render damage to the DNA, particularly due to absorption by the sugar–phosphate backbone. Exposure to vacuum UV radiation (<190 nm) causes fragmentation of DNA.[53,54] Soft ultraviolet (300–400 nm) produces temporary nonlethal inactivation of the *D. radiodurans*, which can recover due to its efficient DNA self-repair mechanisms.[55,56]

In this work, the *D. radiodurans* samples were only slightly affected by the plasma in Martian atmospheric mixture, despite high integral energy radiated by this plasma in the range 140–360 nm. In contrast, damage to the bare DNA was stronger and the DNA removal rates were comparable to those induced by the oxygen plasma.

Therefore, the protective properties of microbial coating membranes successfully prevent penetration of soft UV photons from reaching the genetic DNA, which otherwise, if uncoated, would have been damaged by these emissions. Other bare inner-cell elements, proteins, for example, were also less resistant to plasma exposure then the microbial samples (see Fig. 10). Destruction of the microbes may be achieved either by high-energy photons or highly accelerated ions or by chemically reactive reagents such as oxygen atoms and perhaps metastable O_2^* molecules. Oxygen plasma provides all of these factors combined in a synergetic sterilizing action and is thus more effective.

The better removal efficiency of oxygen relative to the Martian atmospheric mixture demonstrates that, while emission from CO, CO^+, and CO_2^+ may play some role in the degradation process, especially in damaging the bare DNA, the chemical action of atomic oxygen is required to effectively remove the microbe bodies. In terms of microorganism mortality (as opposed to complete removal of biological matter), the ultraviolet radiation from CO, CO^+, and CO_2^+ may conceivably be more effective under certain circumstances than the chemical reactivity of oxygen plasma species. Depending on experimental conditions and microbial culture, the CO_2 plasma may provide faster inactivation rates. This explains the results obtained by several researchers[14,15] who found carbon dioxide to be somewhat superior to oxygen.

In the low-power discharges, production of oxygen from the CO_2 plasma is limited to about 30%,[1] so the decontamination efficiency of the plasma in the Martian atmospheric gas is not expected to be more than 30% of that in oxygen. On the other hand, the plasma ignited directly in the Martian atmosphere might appear to be the easiest means of sterilization on the surface of Mars for sample return purposes, although the sterilization process will take a longer time than in the oxygen plasma. Further research in this direction is necessary.

V. Recommendations

The following recommendations for further research may be suggested. A sterilization plasma can be created directly in Martian atmosphere at natural pressure on the surface of Mars (~700 Pa). We believe that a flowing afterglow plasma can be adequate for in situ removal of biological or organic traces. A convenient design of the sterilization device may have a form of a torch. In this respect, a structure proposed for a torche à injection axiale[57] or other microwave-driven torch design[58] may be utilized. A high-frequency (490-MHz) microfabricated inductively coupled plasma generator[59] or a microwave-powered microstrip plasma device[60] may also be beneficial. Oxygen necessary for faster sterilization may be obtained by plasma-based decomposition of Martian atmosphere.[61] Such a design would involve the initial extraction of oxygen and its accumulation, storage, and then consumption as an agent in the sterilizing plasma. This method would require only low electrical power and no predelivered consumables.

VI. Conclusions

We have thoroughly characterized low-power oxygen plasma in different regimes of operation and compared its sterilization efficiency with that of the plasma in Martian-atmosphere-analog mixture. The combination of diagnostics allowed us to determine signatures of plasma coupling: primary inductive mode, stray capacitive mode, and a transitional state sustained in part inductively with a significant capacitive component. The type of coupling was then monitored using optical emission spectroscopy. The electron and ion densities were significantly larger in the inductive mode as compared to the other regimes of plasma coupling. This resulted in higher rates of all electron-impact-based processes. Greater dissociation, higher UV fluences, higher gas-kinetic temperatures, and greater ion fluxes to the sample surface were the consequences, and there was a reduction in energy of ions striking the surface relative to the capacitive mode. The coupling efficiency and overall power-utilization efficiency were better in the inductively coupled mode.

The plasma with the inductive coupling was found to be more efficient at destroying biological matter than the plasma operated in a capacitive mode at the same applied RF power. The improved efficiency was attributed to several synergetic mechanisms. Oxygen atoms and perhaps metastable O_2^* molecules prompted chemical alteration and volatilization of the biomaterials. This chemical action was complemented by UV photochemistry and ion bombardment. The effect of thermal degradation was minimal. The faster decomposition rates in the inductive mode were accounted for chiefly by the higher density of atomic oxygen available for sample removal.

The chemical reactivity was found to play the primary role in O_2 plasma sterilization under all conditions explored. The flux of highly energetic (far ultraviolet) photons was also important. The oxygen plasma was more efficient than the plasma in Martian-atmosphere-analog mixture. There was a denser concentration of O atoms in the former plasma but stronger integral UV emission at 140–360 nm in the latter. Protective properties of microbial cell coatings and perhaps the DNA self-repair obstructed soft UV photons from damaging the genetic DNA.

Based on our data and results from the reviewed literature, several conclusions can be drawn regarding sterilization mechanisms in plasmas at reduced pressure. Effects of physical sputtering by ion bombardment are rather limited (even for heavy ions, such as Ar^+) but may be a major factor at very low pressure in capacitively coupled plasma. Plasma-generated UV photons are generally more effective at short wavelengths. Far ultraviolet radiation might control the rate of genetic inactivation of isolated microorganisms but is often incapable of sterilizing the aggregated colonies thoroughly. Photodesorption plays a secondary role in plasmas containing any chemically reactive species, but this process may determine the bactericidal properties of plasmas in rare gases. For the oxygen plasma, the fastest sterilization rate is achieved in the regime that provides the highest flux of oxygen atoms to the surface. The metastable species may be especially important in afterglow plasmas (e.g., in a plasma torch). All mechanisms act synergistically; which one is dominant depends on conditions and biological culture.

Acknowledgments

This work was performed while one of the authors (A.A.B.) held a National Research Council Research Associateship Award at NASA Ames Research Center. The work of M.V.V.S.R. and B.A.C. was funded by NASA Ames Contract NAS2-99092 to ELORET Corporation. Jeffery Ifland of ELORET Corp. is acknowledged for his role in constructing the biological degradation reactor.

References

[1] Buser, R. G., and Sullivan, J. J., "Initial Processes in CO_2 Glow Discharges," *Journal of Applied Physics*, Vol. 41, No. 2, 1970, pp. 472–479.

[2]Alfa, M. J., "Methodology of Reprocessing Reusable Accessories," *Gastrointestinal Endoscopy Clinics of North America*, Vol. 10, No. 2, 2000, pp. 361–378.

[3]Moisan, M., Barbeau, J., Moreau, S., Pelletier, J., Tabrizian, M., and Yahia, L., "Low-Temperature Sterilization Using Gas Plasmas: A Review of the Experiments and an Analysis of the Inactivation Mechanisms," *International Journal of Pharmaceutics*, Vol. 226, Nos. 1–2, 2001, pp. 1–21.

[4]Laroussi, M., "Nonthermal Decontamination of Biological Media by Atmospheric-Pressure Plasmas: Review, Analysis, and Prospects," *IEEE Transactions on Plasma Science*, Vol. 30, No. 4, 2002, pp. 1409–1415.

[5]Rutala, W. A., and Weber, D. J., "Infection Control: The Role of Disinfection and Sterilization," *Journal of Hospital Infection*, Vol. 43 (Suppl.), 1999, pp. S43–S55.

[6]Goldman, M., and Pruitt, L., "Comparison of the Effects of Gamma Radiation and Low Temperature Hydrogen Peroxide Gas Plasma Sterilization on the Molecular Structure, Fatigue Resistance, and Wear Behavior of UHMWPE," *Journal of Biomedical Materials Research*, Vol. 40, No. 3, 1998, pp. 378–384.

[7]D'Agostino, R. (ed.), *Plasma Deposition, Treatment, and Etching of Polymers*, Academic Press, Boston, 1990.

[8]Standaert, T. E. F. M., Matsuo, P. J., Li, X., Oehrlein, G. S., Lu, T.-M., Gutman, R., Rosenmayer, C. T., Bartz, J. W., Langan, J. G., and Entley, W. R., "High-Density Plasma Patterning of Low Dielectric Constant Polymers: A Comparison Between Polytetrafluoroethylene, Parylene-N, and Poly(arylene ether)," *Journal of Vacuum Science and Technology A*, Vol. 19, No. 2, 2001, pp. 435–446.

[9]Pons, M., Pelletier, J., Joubert, O., and Paniez, P., "Development of Polymers in O_2 Plasmas: Temperature Effects and Transition to Imperfect Anisotropy," *Japanese Journal of Applied Physics, Part 1*, Vol. 34, No. 7A, 1995, pp. 3723–3730.

[10]Lamontagne, B., Küttel, O. M., and Wertheimer, M. R., "Etching of Polymers in Microwave/Radio-Frequency O_2–CF_4 Plasma," *Canadian Journal of Physics*, Vol. 69, Nos. 3–4, 1991, pp. 202–206.

[11]Reichelderfer, R. F., Welty, J. M., and Battey, J. F., "The Ultimate By-Products of Stripping Photoresist in an Oxygen Plasma," *Journal of the Electochemical Society*, Vol. 124, No. 12, 1977, pp. 1926–1927.

[12]Fraser, S. J., Olson, R. L., and Leavens, W. M., "Plasma Sterilization Technology for Spacecraft Applications," NASA CR-146314, March 1976.

[13]Nelson, C. L., and Berger, T. J., "Inactivation of Microorganisms by Oxygen Gas Plasma," *Current Microbiology*, Vol. 18, No. 4, 1989, pp. 275–276.

[14]Lerouge, S., Wertheimer, M. R., Marchand, R., Tabrizian, M., and Yahia, L'H., "Effect of Gas Composition on Spore Mortality During Low-Pressure Plasma Sterilization," *Journal of Biomedical Materials Research*, Vol. 51, No. 1, 2000, pp. 128–135.

[15]Hury, S., Vidal, D. R., Desor, F., Pelletier, J., and Lagarde, T., "A Parametric Study of the Destruction Efficiency of Bacillus Spores in Low Pressure Oxygen-Based Plasmas," *Letters in Applied Microbiology*, Vol. 26, No. 6, 1998, pp. 417–421.

[16]Subramanyam, T. K., Schwefel, R., and Awakowicz, P., "Plasma Sterilization and Correlation to Plasma Diagnostics," *VIDE—Science Technique et Applications*, Vol. 57, No. 303, 2002, pp. 169–174.

[17]Lisovskiy, V. A., Yakovin, S. D., Yegorenkov, V. D., and Terent'eva, A. G., "Plasma Sterilization in Low-Pressure rf Discharge," *Problems of Atomic Science and Technology*, No. 1, 2000, pp. 77–81.

[18]Boucher, R. M. G., "Seeded Gas Plasma Sterilization Method," U.S. Patent No. 4207286, 10 June 1980.

[19]Moreau, S., Moisan, M., Tabrizian, M., Barbeau, J., Pelletier, J., Ricard, A., and Yahia, L'H., "Using the Flowing Afterglow of a Plasma to Inactivate *Bacillus subtilis* Spores: Influence of the Operating Conditions," *Journal of Applied Physics*, Vol. 88, No. 2, 2000, pp. 1166–1174.

[20]Moisan, M., Barbeau, J., Crevier, M.-C., Pelletier, J., Philip, N., and Saoudi, B., "Plasma Sterilisation. Methods and Mechanisms," *Pure and Applied Chemistry*, Vol. 74, No. 3, 2002, pp. 349–358.

[21]Soloshenko, I. A., Tsiolko, V. V., Khomich, V. A., Shchedrin, A. I., Ryabtsev, A. V., Bazhenov, V. Y., and Mikhno, I. L., "Sterilization of Medical Products in Low-Pressure Glow Discharges," *Plasma Physics Reports [*Translated from *Fizika Plazmy]*, Vol. 26, No. 9, 2000, pp. 792–800.

[22]Philip, N., Saoudi, B, Crevier, M.-C., Moisan, M., Barbeau, J., and Pelletier, J., "The Respective Roles of UV Photons and Oxygen Atoms in Plasma Sterilization at Reduced Gas Pressure: The Case of N_2–O_2 Mixtures," *IEEE Transactions on Plasma Science*, Vol. 30, No. 4, 2002, pp. 1429–1436.

[23]Kastenmeier, B. E. E., Matsuo, P. J., Beulens, J. J., and Oehrlein, G. S., "Chemical Dry Etching of Silicon Nitride and Silicone Dioxide Using $CF_4/O_2/N_2$ Gas Mixtures," *Journal of Vacuum Science and Technology A*, Vol. 14, No. 5, 1996, pp. 2802–2813.

[24]Venkateswaran, A., McFarlan, S. C., Ghosal, D., Minton, K. W., Vasilenko, A., Makarova, K., Wackett, L. P., and Daly, M. J., "Physiologic Determinants of Radiation Resistance in *Deinococcus radiodurans*," *Applied and Environmental Microbiology*, Vol. 66, No. 6, 2000, pp. 2620–2626.

[25]Minton, K. W., "DNA Repair in the Extremely Radioresistant Bacterium *Deinococcus radiodurans*," *Applied and Environmental Microbiology*, Vol. 66, No. 6, 1994, pp. 2620–2626.

[26]Kim, J. S., Rao, M. V. V. S., Cappelli, M. A., Sharma, S. P., and Meyyappan, M., "Mass Spectrometric and Langmuir Probe Measurements in Inductively Coupled Plasmas in Ar, CHF_3/Ar and $CHF_3/Ar/O_2$ Mixtures," *Plasma Sources, Science and Technology*, Vol. 10, No. 2, 2001, pp. 191–204.

[27]Mogul, R., Bol'shakov, A. A., Chan, S. L., Stevens, R. M., Khare, B. N., Meyyappan, M., and Trent, J. D., "Impact of Low-Temperature Plasmas on *Deinococcus radiodurans* and Biomolecules," *Biotechnology Progress*, Vol. 19, No. 3, 2002, pp. 776–783.

[28]Cruden, B. A., Rao, M. V. V. S., Sharma, S. P., and Meyyappan, M., "Detection of Chamber Conditioning by CF_4 in an Inductively Coupled Plasma Reactor," *Journal of Vacuum Science and Technology B*, Vol. 20, No. 1, 2002, pp. 353–363.

[29]Miller, P. A., Hebner, G. A., Greenberg, K. E., Pochan, P. D., and Aragon, B. P., "An Inductively Coupled Plasma Source for the Gaseous Electronics Conference RF Reference Cell," *Journal of Research of the National Institue of Standards and Technology*, Vol. 100, No. 4, 1995, pp. 427.

[30]Schwabedissen, A., Benck, E. C., and Roberts, J. R., "Influence of Different Coil Geometries on the Spatial Distribution of the Plasma Density in Planar Inductively Coupled Plasmas," *Physical Review E*, Vol. 56, No. 5, 1997, pp. 5866–5875.

[31]Cruden, B. A., Rao, M. V. V. S., Sharma, S. P., and Meyyappan, M., "Neutral Gas Temperature Estimates in an Inductively Coupled CF_4 Plasma by Fitting Diatomic Emission Spectra," *Journal of Applied Physics*, Vol. 91, No. 11, 2002, pp. 8955–8964.

[32]Cheah, S.-L., Lee, Y.-P., and Ogilvie, J. F., "Wavenumbers, Strengths, Widths and Shifts with Pressure of Lines in Four Bands of Gaseous $^{16}O_2$ in the Systems $a^1\Delta_g$–$X^3\Sigma_g^-$ and $b^1\Sigma_g^+$–$X^3\Sigma_g^-$," *Journal of Quantitative Spectroscopy and Radiative Transfer*, Vol. 64, No. 5, 2000, pp. 467–482.

[33]Rouille, G., Millot, G., Saint-Loup, R., and Berger, H., "High-Resolution Stimulated Raman Spectroscopy of O_2," *Journal of Molecular Spectroscopy*, Vol. 154, No. 2, 1992, pp. 372–382.

[34]Krupenie, P. H., "The Spectrum of Molecular Oxygen," *Journal of Physical and Chemical Reference Data*, Vol. 1, No. 2, 1972, pp. 423–534.

[35]Watson, J. K. G., "Rotational Line Intensities in $^3\Sigma$–$^1\Sigma$ Electronic Transitions," *Canadian Journal of Physics*, Vol. 46, No. 14, 1968, pp. 1637–1643.

[36]Albritton, D. L., Schmeltekopf, A. L., Harrop, W. J., Zare, R. N., and Czarny, J., "An Analysis of the $O_2^+ b^4\Sigma_g^-$–$a^4\Pi_u$ First Negative Band System," *Journal of Molecular Spectroscopy*, Vol. 67, No. 1–3, 1977, pp. 157–184.

[37]Hill, E., and Van Vleck, J. H., "On the Quantum Mechanics of the Rotational Distortion of Multiplets in Molecular Spectra," *Physical Review*, Vol. 32, 1928, pp. 250–272.

[38]Carl, D. A., Hess, D. W., and Lieberman, M. A., "Oxidation of Silicon in an Electron Cyclotron Resonance Oxygen Plasma: Kinetics, Physicochemical, and Electrical Properties," *Journal of Vacuum Science and Technology A*, Vol. 8, No. 3, 1990, pp. 2924–2930.

[39]Tuszewski, M., Scheuer, J. T., and Tobin, J. A., "Composition of the Oxygen Plasmas from Two Inductively Coupled Sources," *Journal of Vacuum Science and Technology A*, Vol. 13, No. 3, 1995, pp. 839–842.

[40]Lieberman, M. A., and Lichtenberg, A. J., *Principles of Plasma Discharges and Materials Processing*, Wiley, New York, 1994.

[41]Chabert, P., Lichtenberg, A. J., Lieberman, M. A., and Marakhtanov, A. M., "Instabilities in Low-Pressure Electronegative Inductive Discharges," *Plasma Sources, Science and Technology*, Vol. 10, No. 3, 2001, pp. 478–489.

[42]Gudmundsson, J. T., Kouznetsov, I. G., Patel, K. K., and Lieberman, M. A., "Electronegativity of Low-Pressure High-Density Oxygen Discharges," *Journal of Physics D*, Vol. 34, No. 7, 2001, pp. 1100–1109.

[43]Godyak, V. A., Piejak, R. B., and Alexandrovich, B. M., "Probe Diagnostics of Non-Maxwellian Plasmas," *Journal of Applied Physics*, Vol. 73, No. 8, 1993, pp. 3657–3663.

[44]Chen, F. F., "Langmuir Probe Analysis for High Density Plasmas," *Physics of Plasmas*, Vol. 8, No. 6, 2001, pp. 3029–3041.

[45]Gudmundsson, J. T., Marakhtanov, A. M., Patel, K. K., Gopinath, V. P., and Lieberman, M. A., "On the Plasma Parameters of a Planar Inductive Oxygen Discharge," *Journal of Physics D*, Vol. 33, No. 11, 2000, pp. 1323–1331.

[46]Gasnot, L., Desgroux, P., Pauwels, J. F., and Sochet, L. R., "Detailed Analysis of Low-Pressure Premixed Flames of $CH_4 + O_2 + N_2$: A Study of Prompt-NO," *Combustion and Flame*, Vol. 117, No. 1–2, 1999, pp. 291–306.

[47]Williams, B. A., and Fleming, J. W., "Radical Species Profiles in Low-Pressure Methane Flames Containing Fuel Nitrogen Compounds," *Combustion and Flame*, Vol. 110, No. 1–2, 1997, pp. 1–13.

[48]Bochkova, O. P., and Shreider, E. Y., *Spectroscopic Analysis of Gas Mixtures*, Academic Press, New York, 1965.

[49]Leerungnawarat, P., Cho, H., Pearton, S. J., Zetterling, C.-M., and Ostling, M., "Effect of UV Light Irradiation on SiC Dry Etch Rates," *Journal of Electronic Materials*, Vol. 29, No. 3, 2000, pp. 342–346.

[50]Krupenie, P. H., *The Band Spectrum of Carbon Monoxide*, National Bureau of Standards, Washington, DC, 1966.

[51]Hollander, A., and Wertheimer, M. R., "Vacuum Ultraviolet Emission from Microwave Plasmas of Hydrogen and Its Mixtures with Helium and Oxygen," *Journal of Vacuum Science and Technology A*, Vol. 12, No. 3, 1994, pp. 879–881.

[52]Cantor, C. R., and Schimmel, P. R., *Biophysical Chemistry, Part II: Techniques for the Study of Biological Structure and Function*, Freeman, New York, 1980.

[53]Ito, T., "The Effects of Vacuum-UV Radiation (50–190 nm) on Microorganisms and DNA," *Advances in Space Research*, Vol. 12, No. 4, 1992, pp. 249–253.

[54]Hieda, K., Suzuki, K., Hirono, T., Suzuki, M., and Furusawa, Y., "Single-Strand and Double-Strand Breaks in pBR322 DNA by Vacuum–UV from 8.3 to 20.7 eV," *Journal of Radiation Research (Tokyo)*, Vol. 35, No. 2, 1994, pp. 104–111.

[55]Caimi, P., and Eisenstark, A., "Sensitivity of *Deinococcus radiodurans* to Near-Ultraviolet Radiation," *Mutation Research*, Vol. 162, No. 2, 1986, pp. 145–151.

[56]Eisenstark, A., "Mutagenic and Lethal Effects of Near-Ultraviolet Radiation (290–400 nm) on Bacteria and Phage," *Environmental and Molecular Mutagenesis*, Vol. 10, No. 3, 1987, pp. 317–337.

[57]Moisan, M., Sauvé, G., Zakrewski, Z., and Hubert, J., "An Atmospheric Pressure Waveguide-Fed Microwave Plasma Torch: the TIA Design," *Plasma Sources, Science and Technology*, Vol. 3, No. 4, 1994, pp. 584–592.

[58]Jin, Q., Zhu, C., Border, M. W., and Hieftje, G. M., "A Microwave Plasma Torch Assembly for Atomic Emission Spectrometry," *Spectrochimica Acta, Part B*, Vol. 46, No. 3, 1991, pp. 417–430.

[59]Minayeva, O. B., and Hopwood, J. A., "Emission Spectroscopy Using a Microfabricated Inductively Coupled Plasma-on-a-Chip," *Journal of Analytical Atomic Spectrometry*, Vol. 17, No. 9, 2002, pp. 1103–1107.

[60]Engel, U., Bilgic, A. M., Haase, O., Voges, E., and Broekaert, J. A. C., "A Microwave-Induced Plasma Based on Microstrip Technology and Its Use for the Atomic Emission Spectrometric Determination of Mercury with the Aid of the Cold-Vapor Technique," *Analytical Chemistry*, Vol. 72, No. 1, 2000, pp. 193–197.

[61]Vušković, L., Ash, R. L., Shi, Z., Popović, S., and Dinh, T., "Radio-Frequency-Discharge Reaction Cell for Oxygen Extraction from Martian Atmosphere," *SAE Transactions*, Vol. 106, Sec. 1 (*J. Aerospace*), 1997, pp. 1041–1047 (SAE Paper 972499).

G. V. Candler
Associate Editor